Xiao H, Song H, Zhang Y, Qi R, Wang R, Xie Z, et al.. The use of polymeric platinum(IV) prodrugs to deliver multinuclear platinum(II) drugs with reduced systemic toxicity and enhan...

ARTICLE *in* BIOMATERIALS · AUGUST 2012

Impact Factor: 8.56 · DOI: 10.1016/j.biomaterials.2012.08.015 · Source: PubMed

Biomaterials 33 (2012) 8657–8669

Contents lists available at SciVerse ScienceDirect

Biomaterials

journal homepage: www.elsevier.com/locate/biomaterials

The use of polymeric platinum(IV) prodrugs to deliver multinuclear platinum(II) drugs with reduced systemic toxicity and enhanced antitumor efficacy

Haihua Xiao [a,b,1], Haiqin Song [c,1], Yu Zhang [d], Ruogu Qi [a,b], Rui Wang [a,b], Zhigang Xie [a], Yubin Huang [a], Yuxin Li [d], Yin Wu [e,**], Xiabin Jing [a,*]

[a] State Key Laboratory of Polymer Physics and Chemistry, Changchun Institute of Applied Chemistry, Chinese Academy of Sciences, 5625 Renmin Street, Changchun 130022, People's Republic of China
[b] Graduate School of Chinese Academy of Sciences, Beijing 100049, People's Republic of China
[c] Department of Colorectal and Anal Surgery, China-Japan Union Hospital of Jilin University, Changchun 130033, People's Republic of China
[d] National Engineering Laboratory for Druggable Gene and Protein Screening, Northeast Normal University, Changchun 130024, People's Republic of China
[e] Research Center of Agriculture and Medicine Gene Engineering of Ministry of Education, Northeast Normal University, Changchun 130024, People's Republic of China

ARTICLE INFO

Article history:
Received 16 July 2012
Accepted 5 August 2012
Available online 28 August 2012

Keywords:
Amphiphilic copolymer
Drug delivery systems
Micelles
Multinuclear platinum drugs

ABSTRACT

Two dinuclear platinum(IV) prodrugs were prepared from cisplatin and oxaliplatin, and tethered to amphiphilic biodegradable block copolymers. The polymeric dinuclear platinum(IV) prodrugs were allowed to self-assemble into nanomicelles, which showed reduced systemic toxicity, relatively long blood circulation, and enhanced antitumor efficacy. In this way, the bottleneck of present multinuclear platinum drugs, especially their severe systemic toxicity, might be overcome.

1. Introduction

Great efforts have long been made to broaden the clinical spectrum of cisplatin, and to overcome its toxic side effects and acquired drug resistance, many platinum(II) complexes have been synthesized. Among them carboplatin, oxaliplatin and others have been commercialized, but none of them can surpass cisplatin in antitumor activity. It is believed to be due to the fact that pharmacologically all Pt(II) drugs finally form a similar array of DNA adducts to cisplatin [1,2]. Consequently, attention turned to the non-classical platinum complexes, especially multinuclear platinum(II) complexes (**MNPt(II)**s) which contain two or more linked platinum centers, because they can bind to DNA strands in a different manner from cisplatin and its analogs [3–6]. For example, mononuclear platinum drug such as cisplatin binds at the N7 position of both guanine (G) and adenine (A) bases to form interstrand cross-links (1–7%) and intrastrand cross-links (99–93%) via short range (GpG) (47–50%) and (ApG) (23–28%) chelation [7]. Moreover, cisplatin binding produces a rigid bend in DNA of 30–50° directed toward the major groove, and a localized unwinding of the DNA double helix of 13° [7]. In contrast, the DNA binding of **MNPt(II)**s is generally characterized by flexible, non-directional DNA adducts, formation of a greater percentage of interstrand adducts, as well as the ability to form long range DNA adducts and to induce DNA conformational changes to both A- and Z-type DNA [8–11]. It should be noted that global conformational changes such as winding and bending are important features in protein recognition of platinum damaged DNA, and the adducts formed by **MNPt(II)**s are vastly different from the adducts formed by mononuclear platinum drug such as cisplatin and its analogs. Therefore, it has been suggested that the distortions induced by these **MNPt(II)**s are only weakly recognized by DNA repair proteins [12,13]. This results in a systemic bypass allowing the platinum complexes to inhibit DNA transcription and replication [13] and to overcome drug resistance. Therefore, these **MNPt(II)**s represent a completely new paradigm for platinum-based anticancer complexes and appear to offer great potential as new anticancer agents [14].

Based on the in-depth studies on structure–activity relationship of **MNPt(II)**s in cancer cell inhibition, Farrell and co-workers [15]

* Corresponding author. Tel./fax: +86 431 85262775.
** Corresponding author.
E-mail addresses: wuy705@nenu.edu.cn (Y. Wu), xbjing@ciac.jl.cn (X. Jing).
[1] The two first authors of equal contribution to this paper.

0142-9612/$ – see front matter © 2012 Elsevier Ltd. All rights reserved.
http://dx.doi.org/10.1016/j.biomaterials.2012.08.015

outlined some factors which govern the inhibitory capability of the **MNPt(II)**s, e.g., linker chain length between the platinum centers (8 atoms, two ammine and six methylene groups, for example, 1,6-hexanediamine is the best), linker chain flexibility (aliphatic chain linker is much better than aromatic chain), hydrogen-bonding capacity and charge of the linker chain, and the trans-geometry of the chloro ligand to the linking chain.

Unfortunately, though thousands of **MNPt(II)**s have been developed till far, they always exhibit even higher toxicity than cisplatin [16,17]. For example, carboplatin and cisplatin can be administered clinically in a dose of 900 and 60–120 mg/m^2, respectively [1], but phase I trials showed that the maximum tolerated dose (MTD) of the most promising **MNPt(II)** drug, BBR3464, is only 1.1 mg/m^2 [18]. From a recent phase II trial, an even lower MTD of only 0.9 mg/m^2 was reported [19]. Recently it was found that the MTD of another promising **MNPt(II)** drug BBR3571 was ca. 0.25 mg/kg for mice [15]. Therefore, severe toxicity is a dose-limiting factor for **MNPt(II)** drugs. It is a major drawback or a bottleneck of them for clinic use.

Fortunately, developments in new drug delivery systems in last decades provide successful strategies to encapsulate or conjugate drug molecules into polymer micelles. These strategies proved successful in recent years for Pt(II) drugs in reducing their toxicity and improving their efficacy, because the polymer micelles can protect the platinum drugs from rapid blood clearance and prolong their blood circulation time by suppressing the reaction of the platinum drugs with proteins and glutathione (GSH), etc. in blood; the polymer micelles can be taken by cancer cells via endocytosis more rapidly than small molecule platinum drugs by simple molecular diffusion; and the polymer micelles can be used at a high dose level to achieve improved antitumor efficacy but without severe side reactions [20–22].

It is hypothesized that these delivery strategies for mononuclear Pt(II) drugs are also applicable to **MNPt(II)** drugs. When they are delivered in a dosage form of nanoparticles, their toxicity would be greatly reduced and their efficacy could be enhanced. However, to the best of our knowledge, there were few reports on encapsulation or conjugation of **MNPt(II)** drugs, possibly due to the fact that they are difficult either to be encapsulated because most of the **MNPt(II)** drugs are ionic compounds, or to be conjugated onto carrier polymers because they lack in reactive groups such as amino, carboxyl or hydroxyl groups in their molecules. Collins and co-workers [23] encapsulated a di-nuclear Pt(II) drug trans-{[Pt(NH$_3$)$_2$Cl]$_2$ μ-dpzm}$^{2+}$(di-Pt) inside cucurbit uril. The host–guest system showed slow exchange kinetics, did not significantly affect the cytotoxicity of the dinuclear complex, but reactivity of the platinum central ions was reduced. Further in vivo study was not reported.

Inspired by our work on mononuclear cisplatin and oxaliplatin [20,24,25], in this paper, we designed two diPt(IV) complexes derived from cisplatin and oxaliplatin (Scheme 1 and Scheme S1, di-cis-Pt(IV)-COOH, **1**; di-DACH-Pt(IV)-COOH, **2**) with succinato groups on the axial positions of the central Pt ions, and then, the carboxyl groups on the diPt(IV) complexes were allowed to react with pendent amine groups of MPEG-b-PCL-b-PLL to afford polymer-di-Pt(IV) conjugates (Scheme 1 and Scheme S2, polymer/di-cis-Pt(IV), P1 and polymer/di-DACH-Pt(IV), P2), and finally these polymer-diPt(IV) conjugates were assembled into micelles (Scheme 1 and Scheme S2, M1, and M2). It is supposed that the polymer-diPt(IV) micelles can be effectively internalized by cancer cells through endocytosis, providing higher drug concentration

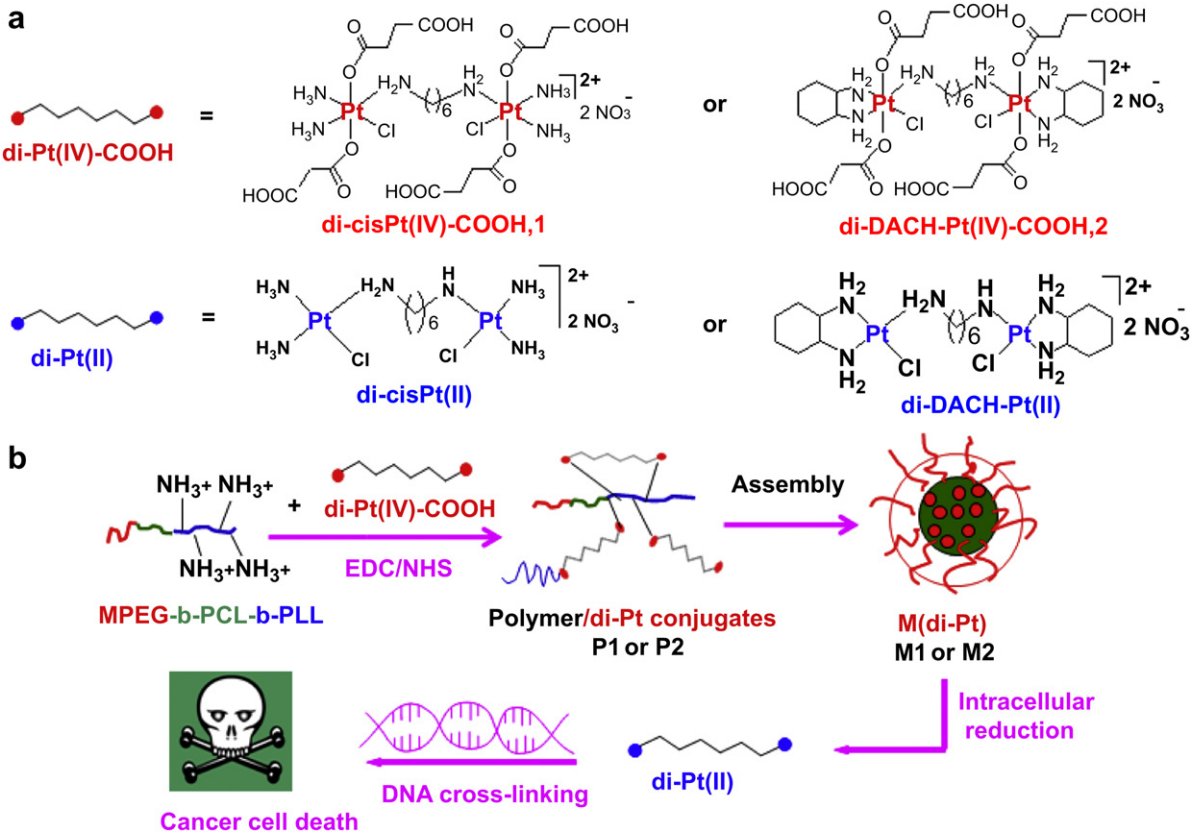

Scheme 1. diPt(IV) prodrugs synthesized (a), schematic preparation of conjugates P1 and P2, and their micelles as well as the possible pathways of drug release as anticancer drugs (b).

than the un-conjugated parental diPt(II) drugs. Once the diPt(IV)-containing micelles come into the endosomes, the lower pH environment and the higher concentration of reducing agents such as GSH and ascorbic acid would facilitate releasing of the highly toxic active anticancer species diPt(II). Thus, the polymer-diPt(IV) micelles can work as prodrugs of diPt(II), but have much lower systemic toxicity and much higher MTD levels.

2. Materials and methods

2.1. Materials

N-hydroxysuccinimide (NHS), 1-ethyl-(3-dimethylaminopropyl)carbodiimide hydrochloride (EDC·HCl), fluorescein isothiocyanate (FITC), sodium ascorbate (NaAsc) and succinic anhydride were purchased from Sigma–Aldrich. Cisplatin (purity 99%), oxaliplatin (purity 99%) and K_2PtCl_4 and 1,2-cyclohexanediamine as well as 1,6-hexanediamine were bought from Shandong Boyuan Pharmaceutical Co. Ltd., China. Preparation and characterization of MPEG-b-PCL-b-PLL were described in our earlier work [20]. All other chemicals and solvents were used without further purification.

2.2. General measurements

^{1}H NMR spectra were measured by a Unity-300 MHz NMR spectrometer (Bruker) at room temperature. Fourier Transform Infrared (FT-IR) spectra were recorded on a Bruker Vertex 70 spectrometer. Mass Spectroscopy (ESI-MS) measurements were performed on a Quattro Premier XE system (Waters) equipped with an electrospray interface (ESI). Inductively Coupled Plasma Optical Emission Spectrometer (ICP-OES, iCAP 6300, Thermoscientific, USA) was used to determine the total platinum contents in the polymer-di-Pt(IV) conjugates and samples obtained outside of the dialysis bags in drug release experiments. Inductively Coupled Plasma Mass Spectrometer (ICP-MS, Xseries II, Thermoscientific, USA) was used for quantitative determination of trace levels of platinum. Size and size distribution of micelles were determined by DLS with a vertically polarized He–Ne laser (DAWN EOS, Wyatt Technology, USA). The morphology of the polymer-diPt(IV) micelles was measured by TEM performed on a JEOL JEM-1011 electron microscope. Particle size and zeta potential measurements were conducted on a Malvern Zetasizer Nano ZS.

2.3. Synthesis of diPt(II) drugs and diPt(IV) drugs

Synthesis and characterization of the platinum drugs di-cisPt(II), di-cisPt(IV)-OH, di-cisPt(IV)-COOH (**1**), di-DACH-Pt(II), di-DACH-Pt(IV)-OH and di-DACH-Pt(IV)-COOH (**2**) were detailed in the Supplementary Information (SI).

2.4. Syntheses of polymer/di-cisPt(IV) and polymer/di-DACH-Pt(IV) conjugates (P1, P2)

Di-cisPt(IV)-COOH (**1**) was conjugated to the polymer MPEG-b-PCL-b-PLL using EDC/NHS method in aqueous solution. Briefly, EDC·HCl (0.191 g, 1 mmol) and NHS (0.115 g, 1 mmol) were dissolved in de-ionized water under stirring. Then **1** (0.31 g, 0.25 mmol) was added into the aqueous solution. Then the polymer MPEG-b-PCL-b-PLL (0.5 g, 0.56 mmol $-NH_2$ groups) in 100 mL water was added and the reaction mixture was kept stirring at room temperature for 24 h, then it was dialyzed against water for 12 h and lyophilized to obtain polymer/di-cisPt conjugates, P1.

Di-DACH-Pt(IV)-COOH (**2**) was conjugated to the polymer MPEG-b-PCL-b-PLL similarly to obtain P2.

2.5. Synthesis of polymer-FITC conjugate (P3)

The polymer MPEG-b-PCL-b-PLL (10 mg) with amino groups was dissolved in water, then FITC was added to the polymer solution. The reaction mixture was kept in dark and stirred for 4 h, dialyzed for 5 days to remove un-reacted FITC, and finally lyophilized to obtain P3.

2.6. Preparation of P1, P2, and (P1 + P3) micelles (M1, M2, and M3)

The micelles of P1 and P2 (coded as M1 and M2, respectively) were prepared by nano-precipitation method. Typically, 50 mg P1 or P2 conjugate was dissolved in a flask with 10 mL DMF, and then 50 mL water was added dropwise into the flask under stirring to form a micellar solution. The solution was dialyzed against water to remove DMF and then freeze-dried.

The composite micelles of P1 + P3 (M3) were prepared in the similar method. 1 mg of conjugate P3 and 9 mg of conjugate P1 were dissolved in 3 mL DMSO in a flask under stirring, and then de-ionized water was dropped into the flask to form composite micelles M3. After that, the micellar solution was dialyzed against water and then freeze-dried.

2.7. Drug release from micelles M1 and M2

5 mg of lyophilized polymer-diPt(IV) micelles (M1, Pt content: 7.75%; M2, Pt content: 10.7%) was dissolved in 5 mL of buffered solutions (100 mM PBS, pH = 7.4; 10 mM acetate buffered solution, pH = 5.0). The solution was then placed into a pre-swollen dialysis bag with a molecular weight cutoff of 3.5 kDa and immersed into 100 mL buffered solution. The dialysis was conducted at 37 °C in a shaking culture incubator. 1.5 mL of sample solution was withdrawn from the incubation medium at specified time intervals and measured for Pt concentration by ICP-OES. After sampling, equal volume of fresh buffered solution was immediately added into the incubation medium. The platinum released from the micelles was expressed as the percentage of cumulative platinum outside the dialysis bag to the total platinum in the micelles. The same drug release procedure was performed in the presence of 5 mM sodium ascorbate aqueous solution.

2.8. XPS study on the reduction of Pt(IV) of P1 in the presence of sodium ascorbate

2.8.1. Instrument

A Thermo ESCALAB 250 X-ray photoelectron spectrometer was used for X-ray photoelectron spectroscopic (XPS) determination (Pt_{4f} and N_{1s}). The analytical conditions were as follows: Al Kα radiation ($h\nu$ = 1486.6 eV) was used as the X-ray source. The pass energy was 20 eV. The analysis chamber was pumped to 5×10^{-6} Pa. The C_{1s} peak at 284.6 eV was chosen for energy calibration.

2.8.2. Sample preparation

(1) Cisplatin, di-cisPt(II) and di-cisPt(IV)-COOH were used for XPS determination directly with desirable amount of drugs;
(2) Di-cisPt(IV)-COOH (1 mM, 5 mL) was incubated with sodium ascorbate (0.5 mM, 5 mL) and then the mixed solution was lyophilized for XPS study;
(3) 50 mg P1 was dissolved in 5 mL water and sodium ascorbate was added to a final concentration of 5 mM. This solution was kept 24 h at room temperature and then it was lyophilized for XPS study.

In all the samples mentioned above, Pt_{4f} and N_{1s} were studied and the results of binding energy were collected in Table 1.

2.9. In vitro study

2.9.1. Cell lines and cell incubation conditions

SKOV-3 (Human ovarian cancer) cells and HCT-8 (human colon cancer) cells were purchased from Institute of Biochemistry and Cell Biology, Chinese Academy of Sciences, Shanghai, China. They were grown in RPMI 1640 (for SKOV-3) and DMEM (for HCT-8) (Life Technologies) supplemented with 10% fetal bovine serum, 0.03% L-glutamine and 1% penicillin/streptomycin in 5% CO_2 at 37 °C, respectively.

2.9.2. Confocal laser scanning microscopy imaging of cancer cells

SKOV-3 cells were grown in RPMI 1640 with 10% fetal bovine serum at 37 °C in 5% CO_2. The cells were seeded in 6-well plates and grown for 24 h prior to incubation with 0.2 mg/mL composite micelles (M3). Live cells were imaged 10 min and 30 min post-treatment.

2.9.3. Determination of platinum contents in the cells

SKOV-3 cells and HCT-8 cells were inoculated in 6-well plates. These cells were then treated with the Pt drugs listed in Table 2 with the Pt concentration in the culture medium regulated to the same value of 5 μM. They were incubated at 37 °C for 2 h or 6 h. After washed with PBS three times, cells were lysed by cell lysis buffer. To quantitatively determine Pt intake by cells [20,21,26], the cell samples were washed three times with ice-cold PBS to remove surface-bound drugs first, and then incubated with 1.5 mL of 0.15 M sodium chloride (pH 3.0 was adjusted by acetic acid) for 3 min at 4 °C, then rinsed with 2 mL of cold PBS, harvested by scraping in ice-cold

Table 1
XPS study of various drugs (Pt_{4f} and N_{1s}).

Sample name	Binding energy (eV)			Pt oxidation state	Kinds of Pt and N
	Pt4f(7/2)	Pt4f(5/2)	N1s		
K_2PtCl_4	73.2	76.4	–	+2	1/0
K_2PtCl_6	75.7	79.0	–	+4	1/0
Cisplatin	72.7	76.2	400.3	+2	1/1
Di-cisPt(II)	73.14	76.5	400.3, 406.7	+2	1/2
Di-cisPt(IV)-COOH	75.6	78.8	400.3, 406.7	+4	1/2
Di-cisPt(IV)-COOH + NaAsc	73.14; 75.6; 78.8		400.3, 406.7	+2, +4	2/2
P1 + NaAsc	72.6	75.8	400.3, 406.7	+2	1/2

Table 2
IC_{50} values of the Pt drugs against SKOV-3 and HCT-8 and intracellular uptake of these drugs by SKOV-3.

Drugs	IC_{50} (μM of Pt)				Pt uptake by SKOV-3 cells (ng Pt)/(mg protein)	
	SKOV-3		HCT-8			
	48 h	72 h	48 h	72 h	2 h	6 h
Cisplatin	17.7	13.2	12.3	6.3	33.8	112
Di-cisPt(II)	21.8	16.3	29.2	10.0	62.0	253
Di-cisPt(IV)-OH	69.7	47.8	75.0	38.6	51.6	208
Di-cisPt(IV)-COOH (**1**)	53.9	26.0	66.3	22.6	44.7	180
M1	10.6	10.9	20.6	16.0	238.0	2145
Oxaliplatin	29.5	25.5	35.2	21.8	19.0	29
Di-DACH-Pt(II)	1.4	0.6	4.7	4.3	53.6	178
Di-DACH-Pt(IV)-OH	45.2	40.1	46.7	44.8	45.4	157
Di-DACH-Pt(IV)-COOH (**2**)	36.4	32.0	48.9	51.6	16.8	83
M2	15.5	8.7	12.4	15.8	266.5	2930

PBS, and finally centrifuged. Thereafter, the cell pellet were lysed by adding 200 μL cell lysis buffer (Promega lysis buffer) and then the cell lysis solution was freezed at −20 °C for 20 min and thawed at room temperature. 100 μL of the cell lysis solution for each sample was used directly to measure the Pt content by ICP-MS. The other 100 μL of the cell lysis solution was used to determine the protein content in each cell sample by using bicinchoninic acid (BCA) protein assay kit (Beyotime Institute of Biotechnology, Shanghai, China) according to previously published data [20,21,27]. The platinum content was expressed as nano-grams of Pt per milligram of total proteins. Results are shown in Table 2.

2.9.4. MTT (3-(4,5-dmethylthiazol-2-yl)-2,5-diphenyltetrazolium bromide) assay

SKOV-3 and HCT-8 cells harvested in a logarithmic growth phase were seeded in 96-well plates at a density of 10^5 cells/well and incubated in RPMI 1640 and DMEM for 24 h, respectively. The medium was then replaced by platinum based drugs listed in Table 2 with cisplatin and oxaliplatin as standards, at a final equivalent Pt concentration from 0.42 to 216 μM. The incubation was continued for 48 and 72 h. Then, 20 μL of MTT solution in PBS with the concentration of 5 mg/mL was added and the plates were incubated for another 4 h at 37 °C, followed by removal of the culture medium containing MTT and addition of 150 μL of DMSO to each well to dissolve the formazan crystals formed. Finally, the plates were shaken for 10 min, and the absorbance of formazan product was measured at 492 nm by a microplate reader.

2.10. In vivo experiments

2.10.1. Animal use

Kunming (KM) mice (6–8 weeks old) were purchased from Jilin University (Changchun, China). All the mice used in this paper were maintained under required conditions (e.g., pathogen-free condition for nude mice) and they had free access to food and water throughout the experiments. Use of them for this study was approved by the Animal Ethics Committee of Changchun Institute of Applied Chemistry, Chinese academy of sciences.

2.10.2. Evaluation on systemic toxicity of Pt drugs

Healthy KM mice (6–8 weeks old) were randomly assigned to 7 groups (a–g). The drug formulations were listed in Table S1. The drug solutions were administered once via the tail vein. The blood sample of each mouse was collected from the retro-orbital plexus into a coagulation-promoting tube (Shandong Nanyou Medical appliance, China) 7 days post administration of the drugs, and then the blood samples were centrifuged at 3000 rpm for 5 min to obtain plasma samples for measuring clinic parameters including alanine aminotransferase (ALT), aspartate aminotransferase (AST), blood urea nitrogen (BUN), and creatine kinase (CK) by an automatic biochemical analyzer (Beckman CX-5 Pro, USA).

2.10.3. Biodistribution

H22 cells (murine hepatocarcinoma cell lines) were purchased from Institute of Biochemistry and Cell Biology, Chinese Academy of Sciences, Shanghai, China, and cultured in RPMI 1640 (Life Technologies, Gaithersburg, MD) containing 10% fetal bovine serum (Life Technologies), 0.03% L-glutamine and 1% penicillin/streptomycin in 5% CO_2 at 37 °C. The mouse H22 xenograft tumor model was developed by subcutaneously injecting 1×10^6 of H22 cells in 0.1 mL PBS into the right flank of KM mice. The tumor nodules were allowed to grow to a volume of ca. 500 mm^3 before injection of the drugs for bio-distribution study. To evaluate the bio-distribution of cisplatin, di-cisPt(II), and M1 in tumor-bearing mice, cisplatin, di-cisPt(II), and M1 at the equal dose of 5 mg Pt/kg for each drug were injected only once into mice (3 mice each group) via tail vein, and 1 h and 12 h later, mice were sacrificed. Blood, organs (heart, liver, spleen, lung, kidneys, muscle), and tumor tissue were harvested, the organs were dissolved in 65% (v/v) nitric acid, and Pt concentrations were measured by ICP-MS.

2.10.4. In vivo anticancer efficacy evaluation and Pt-DNA adducts analysis in the tumor tissue

The KM mice H22 xenograft tumor model was prepared as in Section 2.10.3. When the tumor nodules grew to a volume of ca. 100–200 mm^3, the animals were randomly divided into 10 groups with 8 mice in each group and treated with drug formulations listed in Table 3 by three times of i.v. injection on day 1, 3, and 5, respectively, with the first drug injection day as day 1. Tumor length (major axis of the tumor) and width (minor axis of the tumor) were measured with calipers every other day over a period of 17 d. The tumor volume was calculated using the following equation: Tumor volume (V) = length × width^2/2, as previously described [22]. The tumor volume and relative body weight curves were plotted using the average tumor size and mean relative body weight in each experimental group at various time points.

In order to evaluate the Pt-DNA adducts concentration in the tumor site, another three mice in group a, b, c, e, f, g, h, i in Table 3 were injected twice (at day 1 and day 3) and the drug formulations and dosages were listed in Table 3. In day 4, right at 24 h post the second injection, the mice were sacrificed and the tumor of each mouse was collected. Genomic DNA was separated and purified from the collected solid tumor samples using DNAZOL (Life Technologies, Inc., Grand Island, NY) according to the manufacturer's instruction. The final DNA pellet was air-dried and then dissolved in 0.1 mL distilled water overnight. The next day, the DNA concentration and purity was determined by measuring absorbance at 260/280 nm with a nanodrop UV spectrometer (NanoDrop Technologies, Inc., Wilmington, DE). An aliquot of DNA (60 μL) was digested with 70% nitric acid (64 μL) in a 65 °C water bath overnight. This was diluted with water (776 μL) containing indium and Triton X-100 to achieve a final concentration of 5% acid (final concentration of 1 ppb for indium and 0.05% Triton X-100). The Pt concentration was then determined by inductively coupled plasma mass spectroscopy (ICP-MS).

2.11. Statistical analysis

The data were expressed as mean ± standard deviation (SD). Student's t-test was used to determine the statistical difference between various experimental and control groups. Differences were considered statistically significant at a level of $p < 0.05$.

3. Results and discussion

3.1. Synthesis and characterization of diPt(II) and diPt(IV) complexes

Starting from cisplatin and trans-1,2-hexanediaminoplatinumdichloride (DACH-Pt-Cl_2), two diPt(II) complexes were prepared by partially replacing with one chloride ligand of the starting Pt(II) complexes with $AgNO_3$ and coupling the products with 1,6-hexanediamine (Scheme S1). And they were further oxidized with H_2O_2 into diPt(IV) moieties (di-cisPt(IV)-OH and di-DACH-Pt(IV)-OH), followed by chelation with succinic anhydride to form complex **1** (di-cisPt(IV)-COOH) and **2** (di-DACH-Pt(IV)-COOH). As shown in Fig. S1(A),

Table 3
Drug formulations and doses for measuring Pt-DNA adducts and evaluation of tumor inhibition.

Group	Drug	Dose (mg Pt/kg)	Total mice used	No. of mice for Pt-DNA adducts[a]	No. of mice for tumor inhibition[b]	Death/days
a	Cisplatin	1	11	3	8	0/17
b	Cisplatin	3.25	11	3	8	8/13
c	Di-cisPt(II)	0.25	11	3	8	0/17
d	Di-cisPt(II)	1	8	0	8	0/17
e	di-cisPt(II)	2	11	3	8	8/11
f	M1	0.25	11	3	8	0/17
g	M1	2	11	3	8	0/17
h	M1	3.25	11	3	8	0/17
i	M1	6.5	11	3	8	0/17
j	Saline	0.9% saline	8	0	8	0/17

[a] Three mice were randomly chosen and sacrificed right at 24 h post the second injection of drugs on day 4 for measuring Pt DNA adducts.
[b] Eight mice were used for tumor inhibition study.

di-cisPt(IV)-OH displays a sharp and intense peak at 3460 cm^{-1} (OH stretching) and a strong peak at 540 cm^{-1}(Pt-OH stretch) [28], respectively, compared with di-cisPt(II). After reacting with succinic anhydride, there appear two peaks (1724 cm^{-1} and 1641 cm^{-1}) characteristic of the coordinated carboxyl group (1641 cm^{-1}) and free carboxyl group (1724 cm^{-1}) in complex **1** [28], respectively, confirming the structure of complex **1**. Moreover, all the three diPt complexes (di-cisPt(II), di-cisPt(IV)-OH and di-cisPt(IV)-COOH) have a strong band at 1340–1380 cm^{-1}, which can be attributed to their counter ions nitrate groups (NO_3^-) [29]. In conclusion, comparison of the three FT-IR spectra of di-cisPt(II), di-cisPt(IV)-OH and complex **1** indicates that di-cisPt(IV)-OH has reacted with succinic anhydride to afford **1**. Similar analysis may be made to the FT-IR spectra of di-DACH-Pt(II), di-DACH-Pt(IV)-OH and complex **2** (Fig. S1(B)) to get the same conclusion that **2** has been successfully prepared.

The ^1H NMR of di-cisPt(II), di-cisPt(IV)-OH and complex **1** in D_2O are shown in Fig. S2(A), respectively. Di-cisPt(II) has the characteristic peaks of $-CH_2-$ in 1,6-hexanediamine at 1.25, 1.57, and 2.55 ppm as reported for similar compounds [30]. After it is reacted with H_2O_2 to form di-cisPt(IV)-OH, the chemical shift of $-CH_2-$ in 1,6-hexanediamine moves to 1.31, 1.61, and 2.71 ppm, respectively, and a new chemical shift of $-CH_2-$ which is the typical succinic acid residue appears at 2.49 ppm, supporting the molecular formula of newly synthesized complex **1**. The ^1H NMR of di-DACH-Pt(II), di-DACH-Pt(IV)-OH, and complex **2** in DMSO-d_6 are collected in Fig. S2(B). The chemical shift from 0.97 to 2.56 ppm of di-DACH-Pt(II) can be attributed to the protons in the linker 1,6-hexanediamine between the two Pt species and the protons in the Pt chelator 1,2-cyclohexanediamine. This assignment was based on the chemical shift of protons in 1,2-cyclohexanediame of oxaliplatin [31] and protons in 1,6-hexanediamine of similar dinuclear platinum(II) drugs reported elsewhere [30]. Moreover, when the ^1H NMR of di-DACH-Pt(II) is collected in DMSO-d_6, the chemical shifts of the active amine protons in the 1,2-cyclohexanediamine and the linker 1,6-hexanediamine can be clearly seen at 4.68, 5.01, 5.53 and 5.64 ppm, respectively. This assignment of the active amine protons at 4.68–5.64 ppm is supported by reported results for similar compounds [30,31]. After the oxidation by H_2O_2 of di-DACH-Pt(II) to di-DACH-Pt(IV)-OH, the chemical shifts of the coordinated amine protons moved to a broader band from 5.9 ppm to 7.9 ppm and this movement is the common feature for the amine ligands of Pt atom when Pt(II) was oxidized to Pt(IV) [32]. Moreover, complex **2** which is synthesized by reacting di-DACH-Pt(IV)-OH with succinic anhydride, displays a further shift of the coordinated amine protons to the band 6.4–7.94 ppm. Chemical shift of CH_2 of succinic anhydride residue cannot be clearly seen due to the overlap of the solvent DMSO.

To further confirm the successful synthesis of diPt(IV) complexes, di-cisPt(IV)-OH and complex **1** were dissolved in water and tested by ESI-MS as examples. The results are shown in Fig. S3(A). There is one major peak at $m/z = 356.3$ which can be attributed to the double charged peak of di-cisPt(IV)-OH and a minor peak at $m/z = 774.4$ which is certainly assigned to single charged peak of this compound. Moreover, the simulated isotopic pattern and distribution are nearly the same as the experimental results. This further proves the successful synthesis of di-cisPt(IV)-OH.

At last, complex **1** was analyzed in the same way using ESI-MS (Fig. S3(B)). Similarly, two characteristic peaks at $m/z = 556.3$ and $m/z = 1111.3$ appear in its spectrum. The two peaks can also be assigned to the double charged peak and the single charged peak of this compound.

From the above results of FT-IR, ^1H NMR, ESI-MS, we have sufficient evidence to support successful synthesis of the diPt(IV) complexes **1** and **2**.

3.2. Syntheses of P1 and P2

The two diPt(IV) complexes **1** and **2** consisted of positively charged Pt ions and nitrate counter ions, and were water soluble. After activation with 1-ethyl-3-[3-dimethylaminopropyl] carbodiimide (EDC) and N-hydroxysuccinimide (NHS), they readily formed amide linkages with amine groups on the biodegradable polymer MPEG-b-PCL-b-PLL, resulting in polymer-diPt(IV) conjugates P1 and P2, respectively. The platinum contents in P1 and P2 measured by ICP-OES were 7.75% and 10.7% w/w, respectively.

3.3. Preparation and characterization of M1 and M2 micelles

The tri-block copolymer MPEG-b-PCL-b-PLL had two hydrophilic blocks (MPEG and PLL) and one hydrophobic block (PCL). DiPt(IV) complexes **1** and **2** were soluble in water. When the polymer MPEG-b-PCL-b-PLL was conjugated with **1** and **2** in aqueous medium, the newly formed polymer-diPt(IV) conjugates P1 and P2 could self-assemble into micelles M1 and M2 with the PCL-b-PLL/diPt(IV) as the inner core, and the MPEG block as the hydrophilic shell. TEM and DLS (Fig. 1) were used to characterize the morphology and size of micelles M1 and M2. Results showed that both of them assumed a spherical shape, their mean diameters were 140 nm and 200 nm determined by TEM, respectively, or 160 nm and 230 nm determined by DLS, respectively, and no aggregation was observed.

3.4. Drug release profiles

In vitro drug release experiment demonstrated that the release kinetics of the both micelles showed acid (Fig. 2(A)) and reduction-dependence (Fig. 2(B)), while they were more susceptible to reduction than to acidity. Take micelle M1 as an example, the cumulative platinum released at 9 h was 70% at pH 5.0, but only 53% at pH 7.4; while releasing 70% platinum took only 128 min in 5 mM NaAsc solution. It was similar in the case of micelle M2. According to our previous HPLC-ICP-MS study on the drug releasing mechanism of polymer mononuclear Pt(IV) conjugates, Pt(II) species were released upon reduction. Taking the similarity of mononuclear Pt(IV) and diPt(IV) into consideration, it is natural to deduce that the released Pt species from M1 and M2 would be their diPt(II) counterparts under the intracellular conditions. In other words, M1 and M2 are the polymeric prodrugs of the corresponding diPt(II) drugs.

3.5. Oxidation state of released Pt species

Although we have studied the drug release profiles in terms of platinum amount released, little information was revealed as to oxidation state and ligands to the Pt atoms in their released Pt species. To identify the oxidation state of Pt released, the dialyzate of M1 solution in the presence of 5 mM NaAsc and the reaction product of di-cisPt(IV)-COOH with NaAsc (molar ratio Pt:NaAsc = 1:0.5) were studied by XPS, with cisplatin, di-cisPt(II), and di-cisPt(IV)-COOH as controls. The results are shown in Fig. 3 and the related binding energy data are collected in Table 1. On one hand, the binding energies of Pt_{4f} in cisplatin, di-cisPt(II), the released products from M1 in the presence of NaAsc were identical to those of K_2PtCl_4 (73.2 and 76.4 eV of the 4f(7/2) and 4f(5/2) levels of Pt(II), respectively), but less than those of K_2PtCl_6 (75.7 and 79.0 eV of the 4f(7/2) and 4f(5/2) levels of Pt(IV), respectively [33–35]). Therefore, it is deduced that the central Pt atoms in these complexes are Pt(II). On the other hand, the binding energy Pt_{4f} of di-cisPt(IV)-COOH was identical to those of K_2PtCl_6 (75.7 and 79.0 eV of the 4f(7/2) and 4f(5/2) levels of Pt(IV)), respectively but higher than those of K_2PtCl_4 (73.2 and 76.4 eV of the 4f(7/2) and

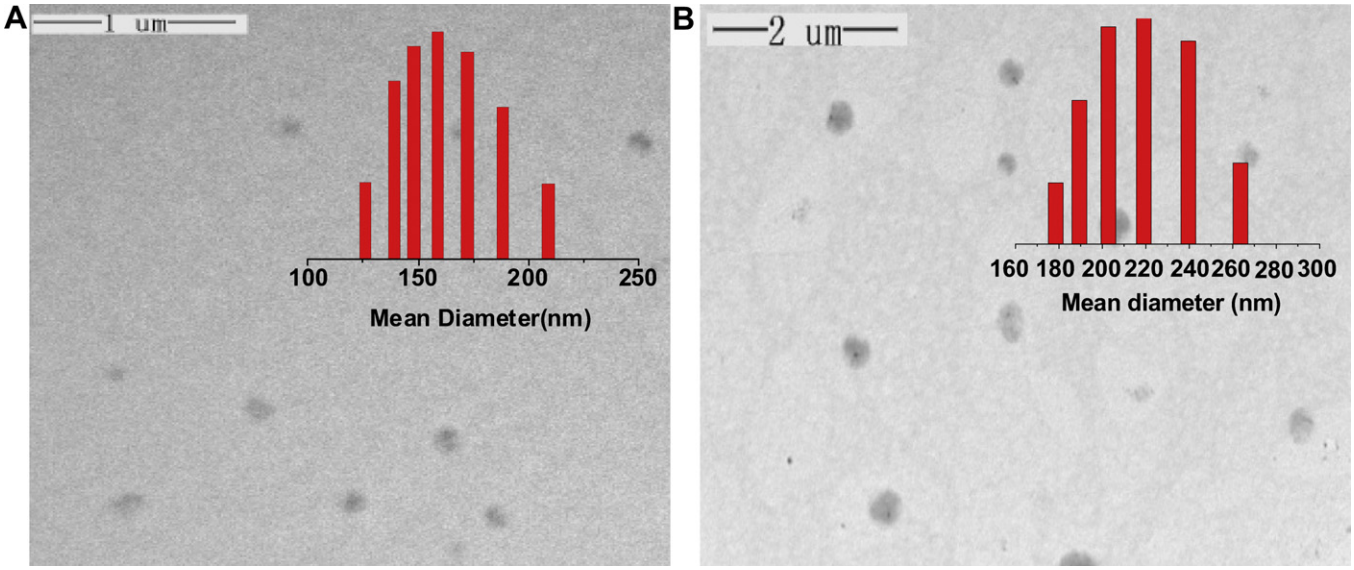

Fig. 1. Characterization of micelles M1 (A) and M2 (B) by TEM and by DLS (insets).

4f(5/2) levels of Pt(II), respectively). Therefore, the oxidation state of Pt in di-cisPt(IV)-COOH is +4. It should be noted that when di-cisPt(IV)-COOH was incubated with insufficient NaAsc for reduction, both Pt(II) and Pt(IV) were obtained as shown in Fig. 3(A, d) where there were three major peaks in Pt_{4f} (73.14, 75.6 and 78.8 eV).

From above discussion, we have every reason to say that the Pt species released from M1 in the presence of enough NaAsc was in +2 valence. Therefore, they can accomplish their mission as anticancer agent.

X-ray photoelectron spectra of N_{1s} (Fig. 3(B)) showed that only one kind of N atom (400.3 eV) exists in cisplatin which can be attributed to the NH_3 ligands, while samples of di-nuclear Pt(II) drugs or dinuclear Pt(IV) drugs possess two kinds of N atoms (a major peak at 400.3 eV and a tiny peak at 406.7 eV) irrespective of the oxidation of Pt atom. Taking the structure of cisplatin and dinuclear platinum(II) as well as dinuclear platinum(IV) compounds into account, it is very easy to assign the major peak of N_{1s} at 400.3 eV to the NH_3 ligand, while the tiny peak at 406.7 eV should be attributed to NH_2 end groups of the linker 1,6-hexadamine coordinated with the two Pt atoms. Correlating the Pt_{4f} spectra with N_{1s} spectra of the dialyzate products of micelle P1 in the presence of NaAsc results in further deduction that the released Pt species were in the form of di-cisPt(II) due to the co-existence of N and Pt similar to the small molecules of di-cisPt(II).

3.6. In vitro cytotoxicity

In vitro MTT assay was used to test the toxicities of micelles M1 and M2 and their parental drugs against SKOV-3 and human corectal cancer HCT-8 at 48 h and 72 h. The results are shown in Figs. 4 and 5. IC_{50} values of each drug were derived and listed in Table 2. For the sake of comparison, platinum concentration was used to express the dosage used and the IC_{50} calculated. As the carrier polymer chosen has proven to be safe in our previous study [20], further measurement on its safety was not performed.

As listed in Table 2, for the cell line of SKOV-3, di-cisPt(II) ($IC_{50,48\ h}$ = 21.8 μM; $IC_{50,72\ h}$ = 16.3 μM) is almost as cytotoxic as cisplatin ($IC_{50,48\ h}$ = 17.7 μM; $IC_{50,72\ h}$ = 13.2 μM), while di-DACH-Pt(II) ($IC_{50,48\ h}$ = 1.4 μM; $IC_{50,72\ h}$ = 0.6 μM) is about twenty times more toxic than oxaliplatin ($IC_{50,48\ h}$ = 29.5 μM; $IC_{50,72\ h}$ = 25.5 μM). When they were oxidized to di-cis-Pt(IV)-OH and di-DACH-Pt(IV)-OH, the toxicity was reduced several times (di-cis-Pt(IV)-OH: $IC_{50,48\ h}$ = 69.7 μM; $IC_{50,72\ h}$ = 47.8 μM; di-DACH-Pt(IV)-OH: $IC_{50,48\ h}$ = 45.2 μM; $IC_{50,72\ h}$ = 40.1 μM). Succination of di-cis-Pt(IV)-OH and di-DACH-Pt(IV)-OH into diPt(IV) complex **1** and **2**, did not change the toxicity significantly. But when complex **1** and **2** were conjugated to carrier polymer, the IC_{50} values decreased several times (M1, $IC_{50,48\ h}$ = 10.6 μM; $IC_{50,72\ h}$ = 10.9 μM; M2, $IC_{50,48\ h}$ = 15.5 μM; $IC_{50,72\ h}$ = 8.7 μM), even less than those of cisplatin and oxaliplatin. This is surely the consequence of conjugation and micellization. As for the HCT-8 cancer cell line, similar results were obtained (Table 2). In short, variation in cytotoxicity of Pt drugs from Pt(II) state to Pt(IV) state and to polymeric PtT(IV) state was similar to that of mononuclear Pt drugs [19–22].

3.7. Intracellular uptake of drugs

Cellular uptake of the micelle M1 by SKOV-3 cells was examined by incubating the cells in the presence of micelle M3 for 10 min and 30 min, and then, imaging the cells by confocal laser scanning microscopy (CLSM). As shown in Fig. 6, green fluorescence of FITC was detected from the plasma part of the cells, its intensity increased from 10 min to 30 min, indicating that the micelles had entered the cells via endocytosis. In order to compare the drug amounts internalized by the cells, ICP-MS was used to determine the platinum content in SKOV-3 cells after they were incubated with various drugs for 2 h and 6 h. The results are shown in Fig. 7. Compared to cisplatin at 6 h (112 (ng Pt)/(mg protein)) [20] and oxaliplatin (29.2 (ng Pt)/(mg protein)), 19 times and 100 times of platinum were uptaken from M1 (2145 (ng Pt)/(mg protein)) and M2 (2930 (ng Pt)/(mg protein)), respectively. It was because polymeric micelles were usually internalized via endocytosis more rapidly than small molecule drugs via simple diffusion through the cell membrane.

3.8. Systemic toxicity

The major drawback of diPt(II) drugs is their higher systemic toxicity and lower MTD. To examine the systemic toxicity of the drugs used, clinic biochemical parameters associated with the function of or damage in liver (ALT, AST), kidneys (BUN, creatinine)

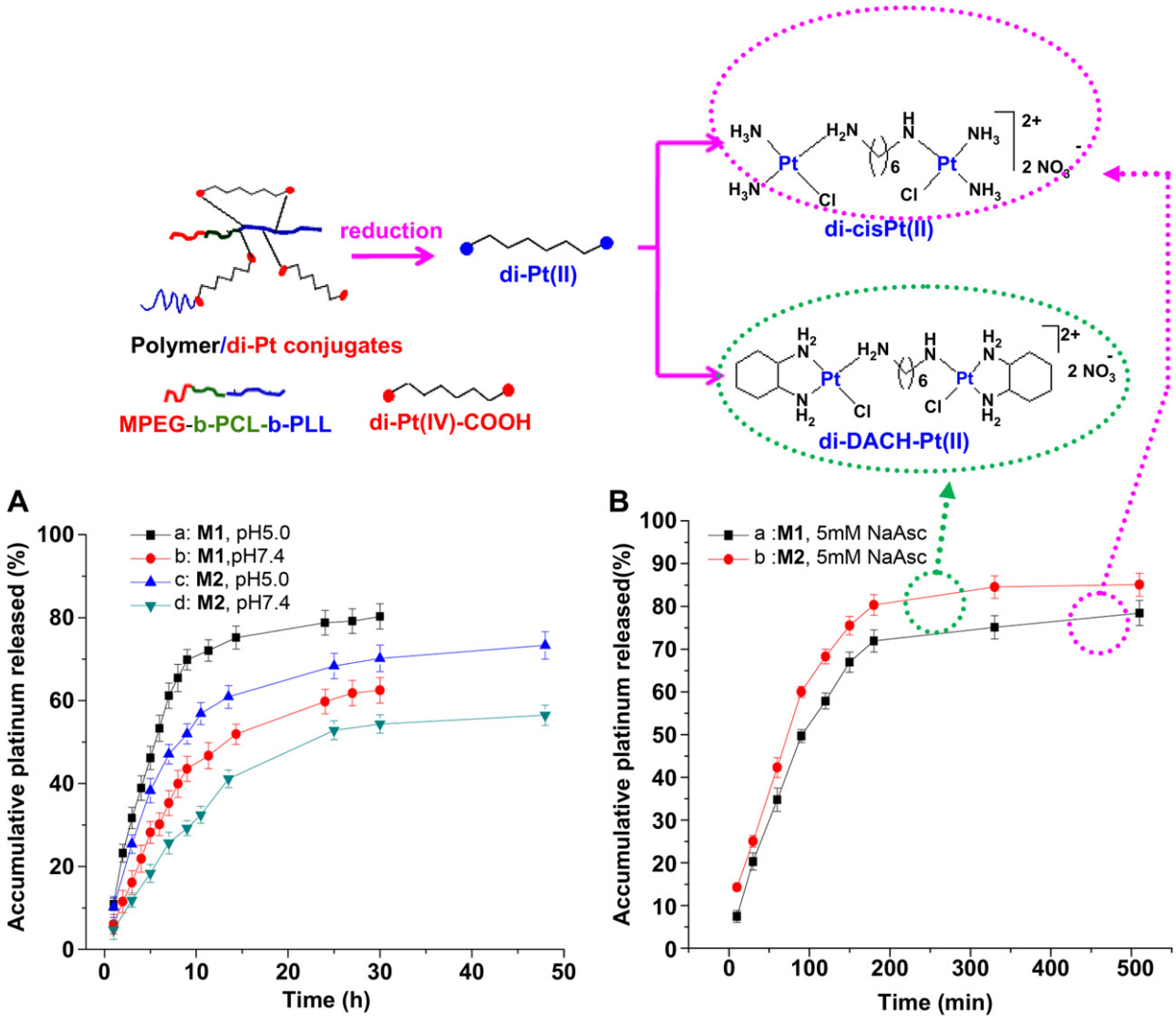

Fig. 2. Drug release profiles of M1 (A(a, b); B(a)) and M2 (A(c, d); B(b)) at pH 5.0 (A(a, c)) and pH 7.4 (A(b, d)) and in the presence of 5 mM sodium ascorbate (NaAsc) aqueous solution (B).

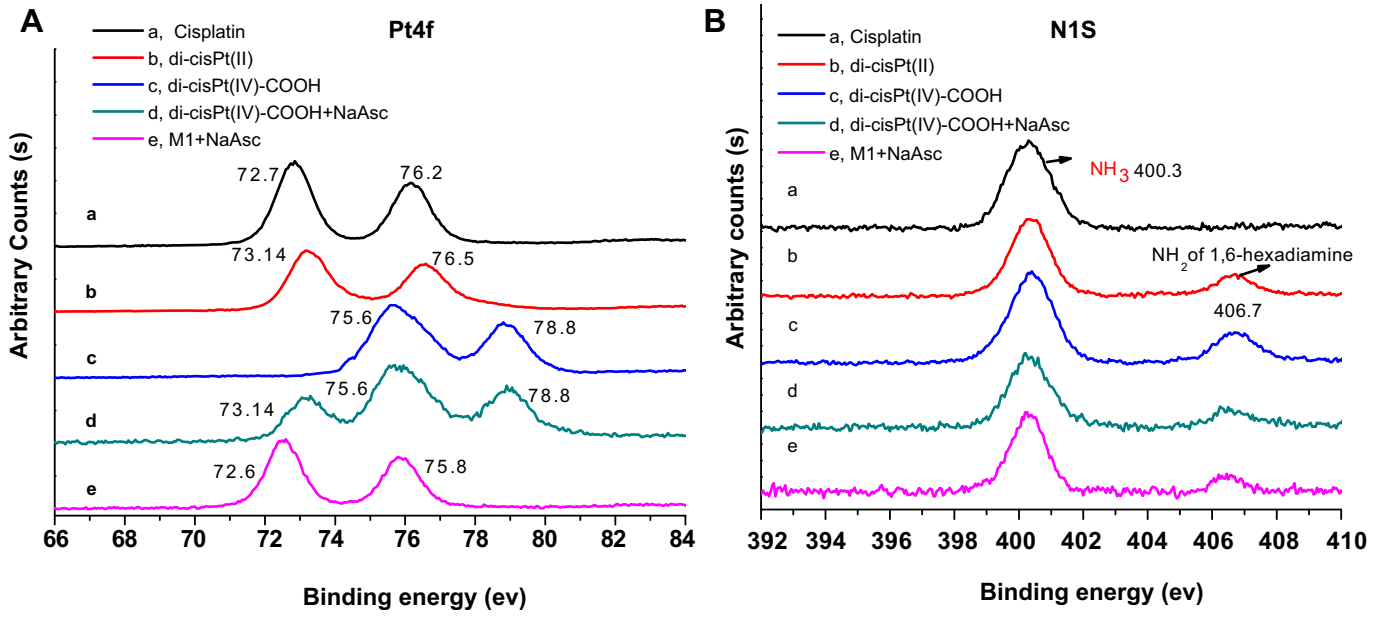

Fig. 3. XPS study of Pt_{4f} (A) and N_{1S} (B) on cisplatin (a), di-cisPt(II) (b), di-cisPt(IV)-COOH (c), the reaction products of di-cisPt(IV) with equimolar NaAsc (d) and the lyophilized dialyzate of M1 in the presence of 5 mM NaAsc (e).

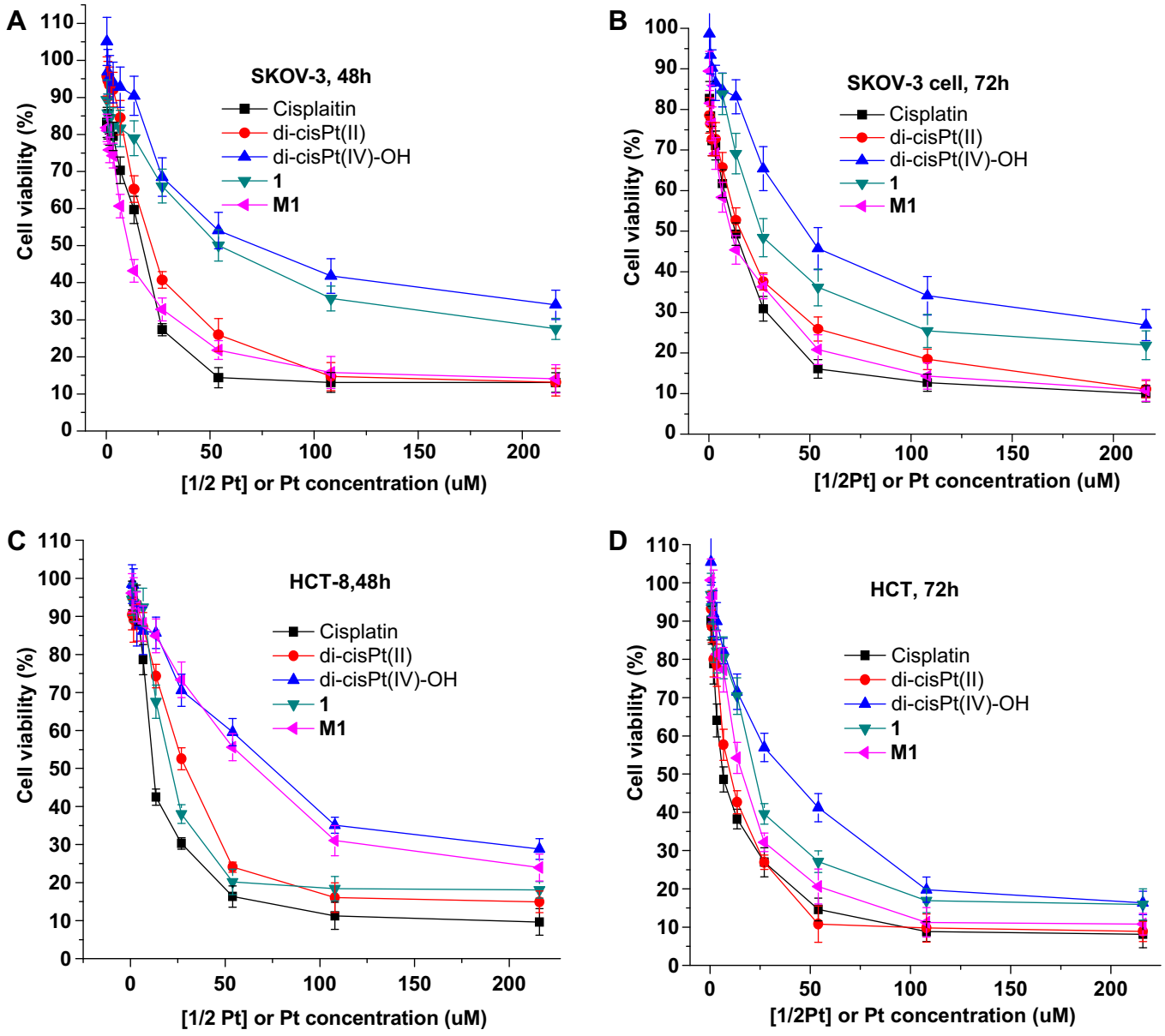

Fig. 4. In vitro cytotoxicity of cisplatin, di-cisPt(II), di-cisPt(IV)-OH, **1** and M1 against SKOV-3 human ovarian cancer cells (A, B) and HCT-8 human colorectal cancer cells (C, D) at 48 h (A, C) and 72 h (B, D).

and heart (CK) were monitored for the mice treated with cisplatin (7.5 and 3.25 mg Pt/kg), di-cisPt(II) (7.5 and 3.25 mg Pt/kg), **1** (7.5 mg Pt/kg) and M1 (7.5 mg Pt/kg) and the results were collected in Fig. 8. Firstly, among the six drug groups tested, all animals in three groups died. They were groups a (cisplatin 7.5 mg Pt/kg), c and d (di-cisPt(II), 7.5 and 3.25 mg Pt/kg, respectively), indicating severe toxicity of these formulations. Compared to the control group g (saline), other three groups displayed deviations in these biochemical parameters and those of group f were the least, indicating the lower systemic toxicity of the M1.

3.9. Biodistribution

Another expectation for polymer-diPt(IV) conjugate is prolongation of blood circulation and possible enrichment in the cancer site. To illustrate these effects, bio-distribution of Pt drugs in blood and organs was studied by ICP-MS. The mice were treated with cisplatin, di-cisPt(II), and M1 at a dose of 5 mg Pt/kg for 1 h and 12 h. As shown in Fig. 9(A), di-cisPt(II) was accumulated mainly in liver and kidneys. This provided explanations for its fast clearance by kidneys, severe nephrotoxicity and hepatotoxicity, and the high mortality in Section 3.8. It is interesting to notice that the Pt concentrations in the tumor site for all the drugs tested increased from 1 h to 12 h, while that in the blood decreased (Fig. 9(B)), indicating there existed a process of partitioning in addition to a process of metabolism and excretion. More interestingly, among the all formulations tested, M1 gave the highest Pt concentration (6.2 μg/g) in tumor at 12 h; it was more than that in liver, kidneys, blood and others except lung (8.5 μg/g). If liver, kidneys or blood is chosen as a reference, this kind of drug distribution can be considered as a targeting effect. Because the micelle M1 does not have a function of active targeting, such targeting effect belongs to passive one due to the enhanced penetration and retention (EPR) effect of the tumor to the polymer-diPt(IV) micelles.

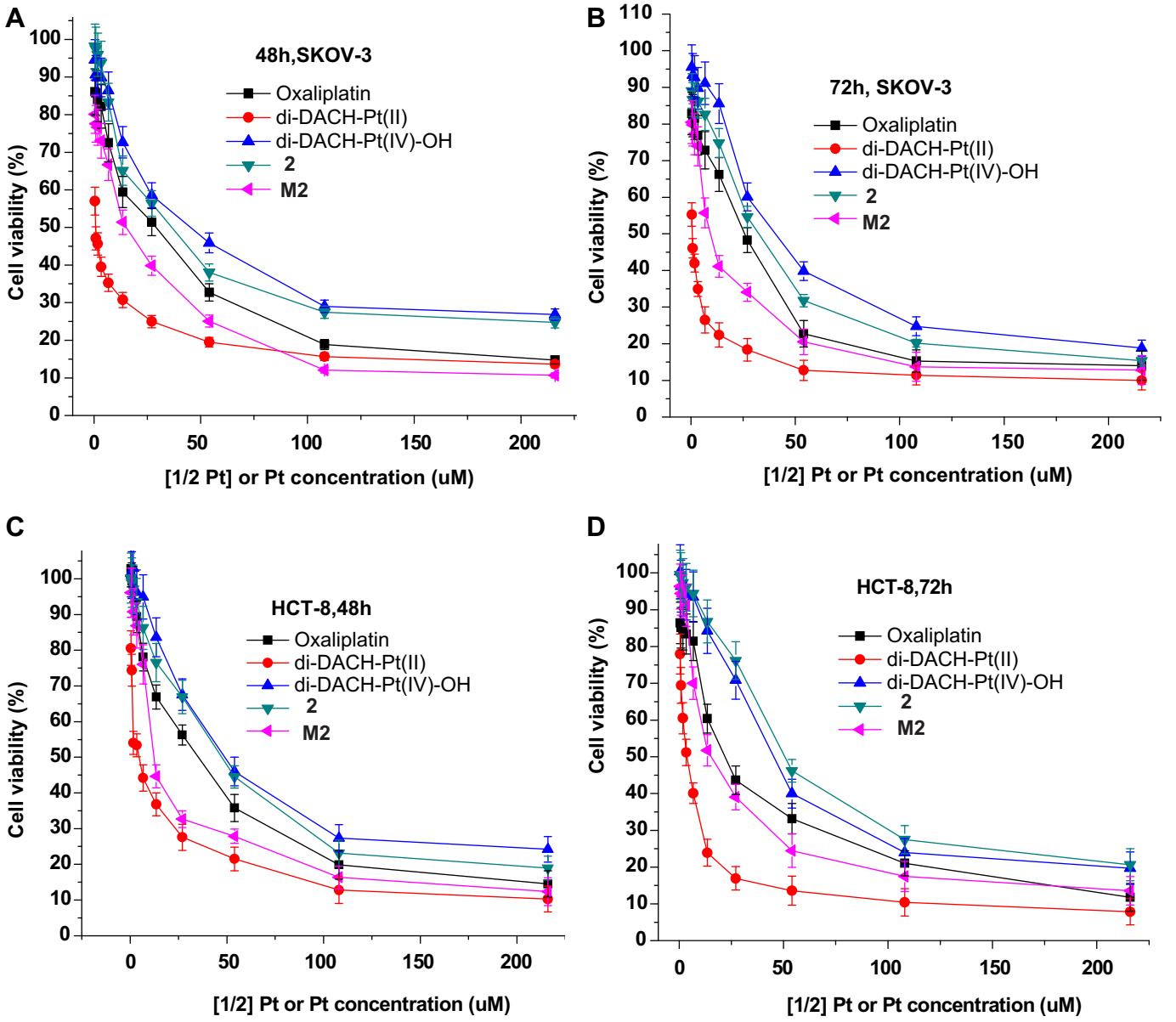

Fig. 5. In vitro cytotoxicity of di-DACH-Pt(II), di-DACH-Pt(IV)-OH, di-DACH-Pt(IV)-COOH and M2 against SKOV-3 human ovarian cancer cells (A, B) and HCT-8 human colorectal cancer cells (C, D) at 48 h (A, C) and 72 h (B, D).

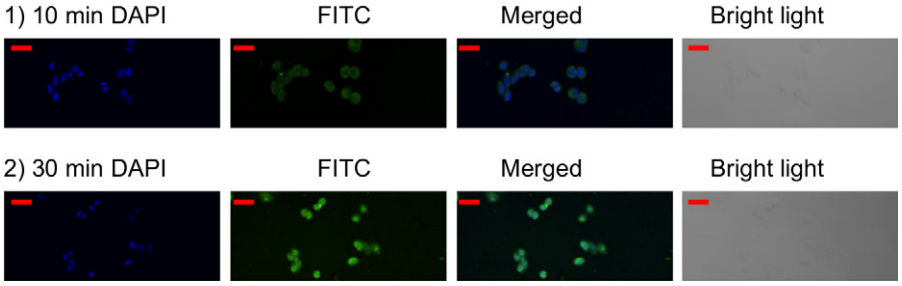

Fig. 6. CLSM images of SKOV-3 cancer cells after 10 min and 30 min incubation with composite micelle M3. Blue fluorescence is from the nuclei stained with 4′,6-diamidino-2-phenylindole (dapi); green fluorescence is from the composite micelles (FITC). (Bars: ▬ =10 μm) (For interpretation of the references to color in this figure legend, the reader is referred to the web version of this article.)

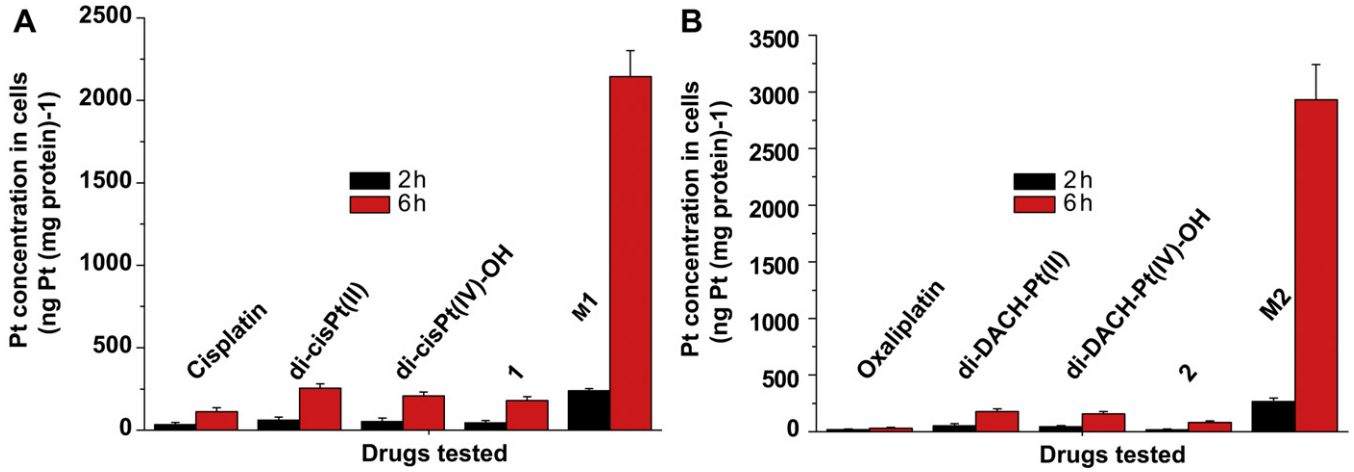

Fig. 7. The intracellular uptake of cisplatin based Pt drugs (A) and oxaliplatin based Pt drugs (B) by SKOV-3 cancer cells 2 h and 6 h post treatment. (Pt concentration in the cells is determined by ICP-MS).

3.10. *In vivo antitumor efficacy*

For better illustrating the advantage of the strategy of polymeric diPt(IV) micelles, in vivo evaluation of M1 was carried out using a H22 (murine hepatocarcinoma) xenograft model developed by injecting H22 cancer cells in the right hand of KM mice. Five days after inoculation of the cancer cells, the tumors were about 100–200 mm^3 in size, and the tumor-bearing mice were randomly divided into 10 groups (8 mice in each group for tumor inhibition study) and were given three i.v. injections of cisplatin, di-cisPt(II) and M1 at desired doses (Table 3) on day 1, 3 and 5, with the day of the first injection counted as day 1. The tumor size and body weight were then monitored every two days for 17 days.

Fig. 10 depicts variation of tumor volume post first injection of drugs. It can be first noted that the mice in group **b** (cisplatin, 3.25 mg Pt/kg) and group **e** (di-cisPt(II), 2 mg Pt/kg), unfortunately, all died in the initial 13 days and 11 days, respectively. Thus, further data could not be obtained. Probably these mice died of acute nephrotoxicity because cisplatin and di-cisPt(II) are highly accumulated and excreted in kidneys as demonstrated by abnormal biochemical parameters in Fig. 8 and in the biodistribution study (Fig. 9). These results indicate that cisplatin and di-cisPt(II) are too toxic to be used at these doses and di-cisPt(II) is even more toxic than cisplatin (lower dose and earlier deaths in group e). This is in agreement with earlier reports [15–19] and this is the major bottleneck of diPt(II)s. Therefore, it is necessary and essential to find a way to reduce the systemic toxicity of diPt(II) drugs and to deliver them into the cancer cells safely.

It is noticed that compared with the control group (group j), group f (M1 at 0.25 mg Pt/kg) show little effect on tumor inhibition ($p > 0.05$). This is possibly due to such a low dose of M1. Under curves j and f come four curves of group a (cisplatin, 1 mg Pt/kg), c

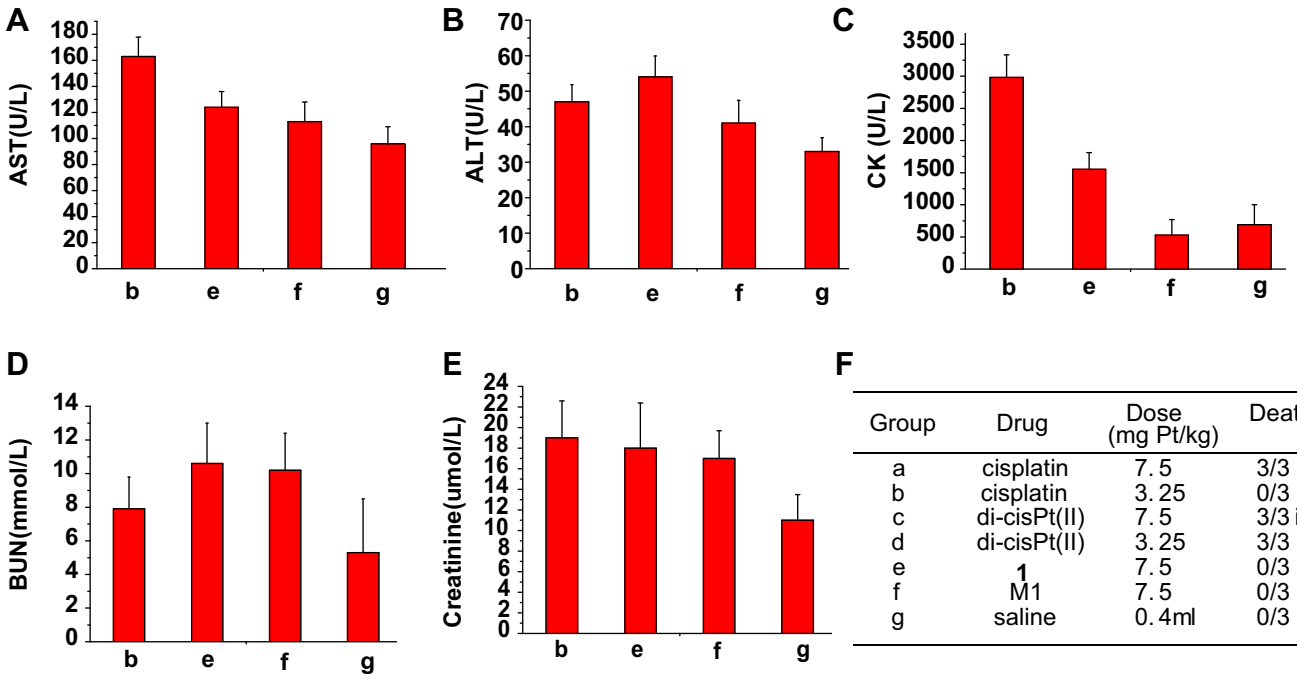

F

Group	Drug	Dose (mg Pt/kg)	Death
a	cisplatin	7.5	3/3 in 4d
b	cisplatin	3.25	0/3
c	di-cisPt(II)	7.5	3/3 in 2d
d	di-cisPt(II)	3.25	3/3 in 5d
e	1	7.5	0/3
f	M1	7.5	0/3
g	saline	0.4ml	0/3

Fig. 8. Variations of clinical parameters (AST, ALT, CK, BUN, creatinine) of the mice treated with various drugs.

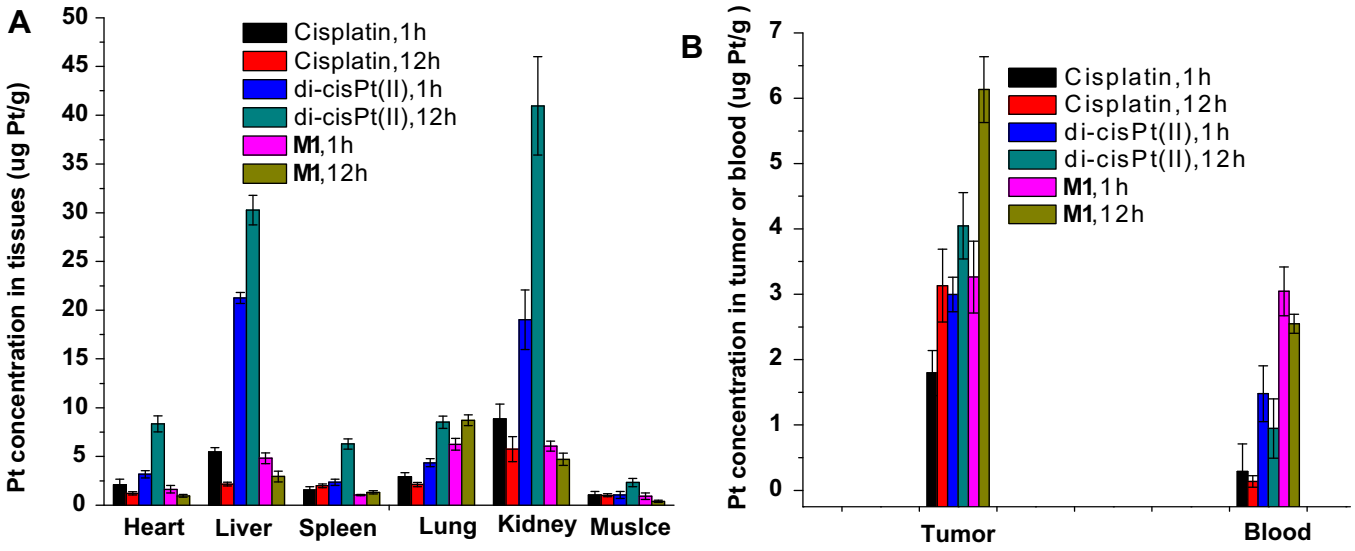

Fig. 9. Biodistribution of Pt drugs in heart, liver, spleen, lung, kidney (A), tumor, and blood (B).

(di-cisPt(II), 0.25 mg Pt/kg), g (M1, 2 mg Pt/kg) and h (M1, 3.25 mg Pt/kg). There is no significant difference among them in the former 11 days ($p > 0.05$). Similarity between these four groups implies that to achieve comparable tumor suppression with cisplatin, less di-cisPt(II) may be used while more M1 should be used, i.e., their anti-tumor capability is in an order of di-cisPt(II) > cisplatin > M1.

Curve h was different from the other three (a, c, g) in that the tumor volume of mice in this group increased more slowly until the end of the test. Because group g and h differ only in dosage, the difference in these two curves reveals the dose-dependence of the antitumor efficacy of M1.

Thereafter are curves d (di-cisPt(II), 1 mg Pt/kg) and i (M1, 6.5 mg Pt/kg). As far as tumor inhibition is concerned, these two groups did not make significant difference from each other under the experimental conditions. Once again here, more M1 achieved the same tumor suppression as less di-cisPt(II).

Overall comparison among M1 groups reveals obvious dose-dependence of the tumor inhibition of M1, from comparable to saline (group f) to most efficacious (group i) among all recipe tested. The examined dose window was from 0.25 to 6.5 mg Pt/kg. Sure enough, di-cisPt(II) series exhibited comparable tumor inhibition with M1 series at a dose from 0.25 to 1 mg Pt/kg (group c and d), dose increase to 2 mg Pt/kg (group e) caused death of all test animals in the first 11 days. That is to say, the effective dose was very close to the MTD of di-cisPt(II). Therefore, clinical use of di-cisPt(II) is impossible. In contrast, by adjusting the dosage of M1 in its safety window, efficacious tumor inhibition can be achieved. Based on the data obtained in the present study, the MTD of M1 should be much more than 6.5 mg Pt/kg.

Fig. 10(B) depicts relative body weight changes of the mice during the test. Among all test groups, group b (cisplatin, 3.25 mg Pt/kg) and group e (di-cisPt(II), 2 mg Pt/kg) mice showed serious weight loss (especially for group e) and all died in the initial 13 and 11 days, respectively, due to the highest systemic toxicity. Group d (di-cisPt(II), 1 mg Pt/kg) mice also showed significant body weight loss in the first 9 days, and after that, they gained their body weight slowly. In all other groups, mice had little weight loss and even gained the body weight constantly because of the lower systemic toxicity.

If groups a to b, groups c to e, and groups h to i were compared, evident dose dependant systemic toxicity could be found. Slightly increasing the drug injection dose of cisplatin and di-cisPt(II), especially for the latter, resulted in severe damage to animals. This was the major drawback of cisplatin and diPt(II)s. In contrast, M1 showed a wider safety window as far as animal body weight was concerned.

In summary, M1 at a dose of 6.5 mg Pt/kg or a little bit more is the most effective and safe enough drug formulation for the xenograft H22 cancer tumor model.

An effective drug delivery system must not only deliver the drug to the cancer cells but also ensure the interaction of the drug with the proper organelles in the cancer cells. DNA is supposed to be the final intracellular target of platinum drugs. The amount of platinum-DNA adducts in the cancer cells is believed to be a measure of the effectiveness of the platinum drug [3–6]. Therefore, three mice in each group were sacrificed right at 24 h post the second injection of drugs on day 4 for measuring Pt-DNA adducts. The tumor tissue was harvested; the tumor cells were collected; all DNAs in the tumor cells were separated and purified; and the platinum content in the "total DNA" was determined by inductively coupled plasma mass spectroscopy (ICP-MS) as a measure of the Pt-DNA adducts formed. As shown in Fig. 10(C) and Table 3, all the drugs tested (cisplatin (a–b), di-cisPt(II) (c–e) and M1 (f–i)) displayed a dose-dependent amount of Pt-DNA adducts, high doses of drugs resulting in high level of Pt-DNA adducts. This can be also used to explain the dose-dependent antitumor effect of these drugs in Fig. 10(A). It is noticed that among group a (cisplatin, 1 mg Pt/kg, 8.5 pg Pt/μg DNA), group e (di-cisPt(II), 2 mg Pt/kg, 6.27 pg Pt/μg DNA), and group g (M1, 2 mg Pt/kg, 9.4 pg Pt/μg DNA), group e showed the least Pt-DNA adducts (Fig. 10(C)), but the highest inhibition to tumor growth (Fig. 10(A)), indicating that the Pt-DNA adducts formed by dinuclear platinum drug di-cisPt(II) are more effective than those formed by mononuclear platinum drug cisplatin. This may be attributed to the different nature of Pt-DNA adducts formed as previously described [3–6]. Group g and group e were given the same amount of Pt (2 mg/kg), but group g showed higher level of Pt-DNA adducts, probably due to the more efficient uptake of the micelles. Furthermore, when the dose was increased to 6.5 mg Pt/kg in group i, the Pt-DNA adducts formed were the most (17.1 pg Pt/μg DNA), corresponding to the best antitumor efficacy of group i (M1, 6.5 mg Pt/kg) (Fig. 10(A)). However, further increasing dose is impossible for di-cisPt(II) due to its systemic toxicity. In other words, micellar drugs can be used in higher dosage to enhance the antitumor efficacy without serious side effects. In this sense, M1 overwhelms both cisplatin and di-cisPt(II).

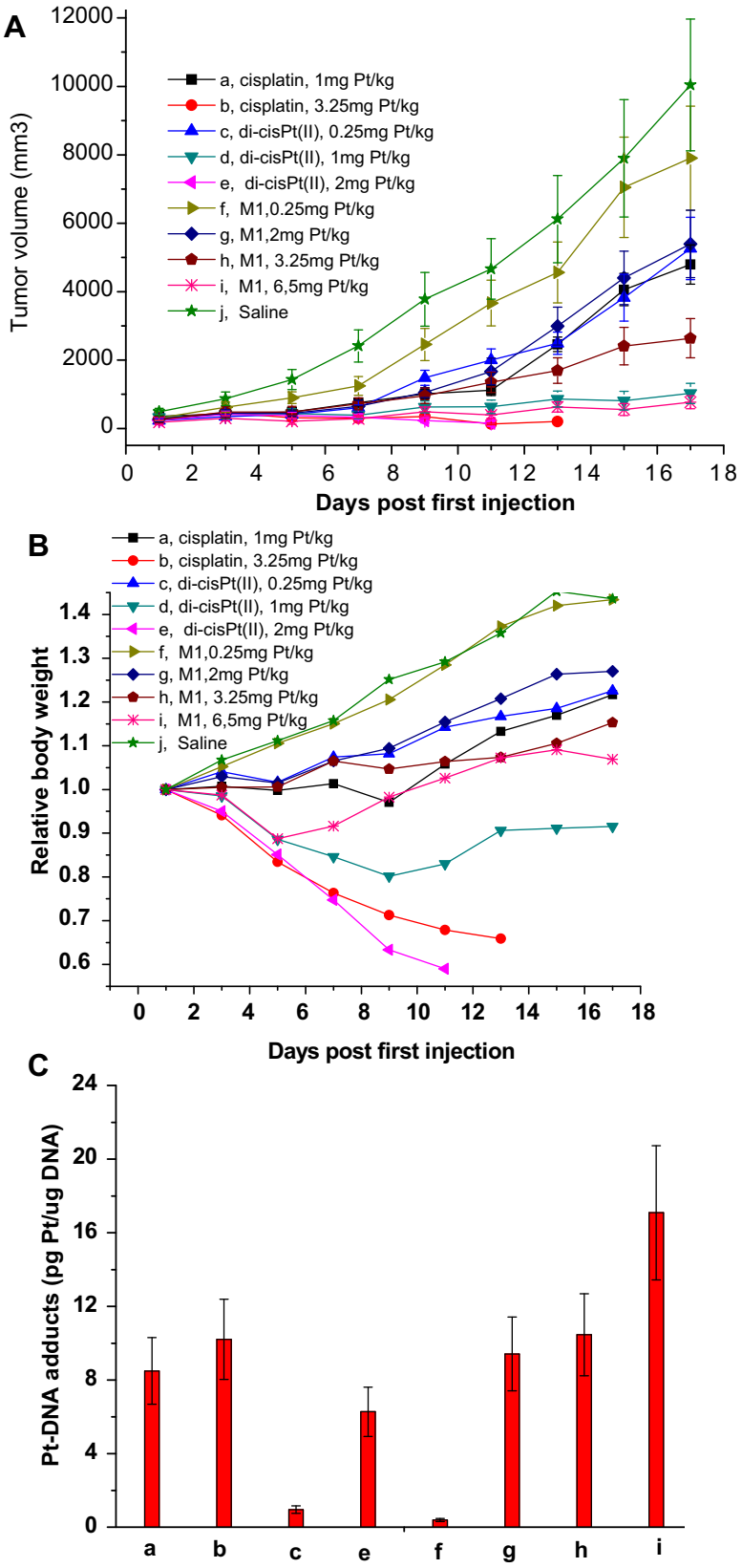

Fig. 10. (A) Effect of (a) cisplatin (1 mg Pt/kg, $n = 8$), (b) cisplatin (3.25 mg Pt/kg, $n = 8$) (c) di-cisPt(II) (0.25 mg Pt/kg, $n = 8$), (d) di-cisPt(II) (1 mg Pt/kg, $n = 8$), (e) di-cisPt(II) (2 mg Pt/kg, $n = 8$), (f) M1 (0.25 mg Pt/kg, $n = 8$), (g) M1 (2 mg Pt/kg, $n = 8$), (h) M1 (3.25 mg Pt/kg, $n = 8$), (i) M1 (6.5 mg Pt/kg, $n = 8$), (j) blank control (0.9% saline, $n = 8$) on the growth of H22 tumors inoculated in KM mice. Each formulation was administered on day 1, 3, and 5 by intravenous injection, with the day of the first injection counted as day 1. Mean values and standard errors of the mean are presented; (B) Body weight changes with time of H22 tumor-bearing mice; (C) Pt-DNA adducts measured right at 24 post the second injection of drugs in group (a–c) and group (e–i).

4. Conclusion

In summary, we have shown a way of delivering polymer-diPt(IV) conjugate micelles as a prodrug of diPt(II). They can be effectively internalized by cancer cells through endocytosis, and thus provide higher intracellular platinum concentration than parental drug diPt(II). Once the diPt(IV) micelles come into the endosomes, the lower pH environment and the higher concentration of reducing agents facilitate release of diPt(II) species, by reduction and concomitant loss of the axial ligands by which they are tethered to the carrier polymer. Thus, the polymer-diPt(IV) conjugate can work as diPt(II)'s prodrug, prolong blood circulation, enhance the drug accumulation at the tumor site, and eventually enhance drug efficacy and reduce side effects at the same time. The polymeric prodrug strategy and endosomal release of anticancer effective di-cisPt(II) drugs can be generally applied to other **MNPt(II)**s. It may be further used in clinical trials to reduce side effects of **MNPt(II)**s and enhance their efficacy.

Acknowledgments

Financial support was provided by the National Natural Science Foundation of China (Project No. 21004062, 51103148), and by the Ministry of Science and Technology of China ("973 Project", No. 2009CB930102); This research was also supported by the National Natural Science Foundation of China (Nos. 31170324 and 31070318), the Fundamental Research Funds for the Central Universities, grants from the Jilin Province Science & Technology Committee, China (Nos. 20100911 and 20110938).

Appendix A. Supplementary data

Supplementary data related to this article can be found at http://dx.doi.org/10.1016/j.biomaterials.2012.08.015.

References

[1] Wong E, Giandomenico CM. Current status of platinum-based antitumor drugs. Chem Rev 1999;99:2451–66.
[2] Kostova I. Platinum complexes as anticancer agents. Recent Pat Anti Canc Drug Discov 2006;1:1–22.
[3] Wheate NJ, Collins JG. Multi-nuclear platinum complexes as anti-cancer drugs. Coord Chem Rev 2003;241:133–45.
[4] Mellish KJ, Qu Y, Scarsdale N, Farrell N. Effect of geometric isomerism in dinuclear platinum antitumour complexes on the rate of formation and structure of intrastrand adducts with oligonucleotides. Nucleic Acids Res 1997;25:1265–71.
[5] Farrell NP, de Almeida SG, Skov AK. Bis(platinum) complexes containing two platinum cis-diammine units. Synthesis and initial DNA-binding studies. J Am Chem Soc 1988;110:5018–9.
[6] Komeda S, Moulaei T, Woods KK, Chikuma M, Farrell NP, Williams LD. A third mode of DNA binding: phosphate clamps by a polynuclear platinum complex. J Am Chem Soc 2006;128:16092–103.
[7] Lippard SJ. Biological processing of DNA modified by platinum compounds. In: Lippard SJ, editor. Progress in inorganic chemistry, bioinorganic chemistry. Sydney: Wiley; 1995. p. 477–516.
[8] Brabec V, Kasparkova J, Vrana O, Novakova O, Cox JW, Qu Y, et al. DNA modifications by a novel bifunctional trinuclear platinum phase I anticancer agent. Biochemistry 1999;38:6781–90.
[9] Johnson A, Qu Y, Van Houten B, Farrell N. B-Z DNA conformational changes induced by a family of dinuclear bis(platinum) complexes. Nucleic Acids Res 1992;20:1697–703.
[10] McGregor TD, Balcarova Z, Qu Y, Tran MC, Zaludova R, Brabec V, et al. Sequence-dependent conformational changes in DNA induced by polynuclear platinum complexes. J Inorg Biochem 1999;77:43–6.
[11] McGregor TD, Bousfield W, Qu Y, Farrell N. Circular dichroism study of the irreversibility of conformational changes induced by polyamine-linked dinuclear platinum compounds. J Inorg Biochem 2002;91:212–9.
[12] Farrell N. DNA binding and chemistry of dinuclear platinum complexes. Comments Inorg Chem 1995;16:373–89.
[13] Kasparkova J, Mellish KJ, Qu Y, Brabec V, Farrell N. Site-specific d(GpG) intrastrand cross-links formed by dinuclear platinum complexes, bending and NMR studies. Biochemistry 1996;35:16705–13.
[14] Pratesi G, Perego P, Polizzi D, Righetti SC, Supino R, Caserini C, et al. A novel charged trinuclear platinum complex effective against cisplatin-resistant tumours: hypersensitivity of p53-mutant human tumour xenografts. Br J Cancer 1999;80:1912–9.
[15] Farrell N. Polynuclear charged platinum compounds as a new class of anticancer agents. In: Kelland LR, Farrell NP, editors. Platinum-based drugs in cancer therapy. Totowa: Humana Press; 2000. p. 321–38.
[16] Wheate NJ, Walker S, Craig GE, Oun R. The status of platinum anticancer drugs in the clinic and in clinical trials. Dalton Trans 2010;39:8113–321.
[17] Wheate NJ, Collins JG. Multi-nuclear platinum drugs: a new paradigm in chemotherapy. Curr Med Chem Anti Canc Agents 2005;5:267–9.
[18] Calvert PM, Highley MS, Hughes AN, Plummer ER, Azzabi AST, Verrill MW, et al. A phase I study of a novel, trinuclear, platinum analogue, BBR3464, in patients with advanced solid tumors. Clin Cancer Res 1999;5:3796s.
[19] Jodrell DI, Evans TR, Steward W, Cameron D, Prendiville J, Aschele C, et al. Phase II studies of BBR3464, a novel tri-nuclear platinum complex, in patients with gastric or gastro-oesophageal adenocarcinoma. Eur J Cancer 2004;40:1872–7.
[20] Xiao H, Qi R, Liu S, Hu X, Duan T, Zheng Y, et al. Biodegradable polymer-cisplatin(IV) conjugate as a pro-drug of cisplatin(II). Biomaterials 2011;32:7732–9.
[21] Duong HTT, Huynh VT, de Souza P, Stenze MH. Core-cross-linked micelles synthesized by clicking bifunctional Pt(IV) anticancer drugs to isocyanates. Biomacromolecules 2010;11:2290–9.
[22] Dhar S, Kolishetti N, Lippard SJ, Farokhzad OC. Targeted delivery of a cisplatin prodrug for safer and more effective prostate cancer therapy in vivo. PNAS 2011;108:1850–5.
[23] Wheate NJ, Day AI, Blanch RJ, Arnold AP, Cullinane C, Collins JG. Multi-nuclear platinum complexes encapsulated in cucurbit[n]uril as an approach to reduce toxicity in cancer treatment. Chem Commun 2004;12:1424–5.
[24] Xiao H, Song H, Yang Q, Cai H, Qi R, Yan L, et al. A prodrug strategy to deliver cisplatin(IV) and paclitaxel in nanomicelles to improve efficacy and tolerance. Biomaterials 2012;33:6507–19.
[25] Xiao H, Li W, Qi R, Yan L, Wang R, Liu S, et al. Co-delivery of daunomycin and oxaliplatin by biodegradable polymers for safer and more efficacious combination therapy. J Control Release. http://dx.doi.org/10.1016/j.jconrel.2012.06.004. Available from: http://www.sciencedirect.com/science/article/pii/S016836591200497X; 2012.
[26] Hamelers IHL, Staffhorst RWHM, Voortman J, de Kruijff B, Reedijk J, van Bergen en Henegouwen PMP, et al. High cytotoxicity of cisplatin nanocapsules in ovarian carcinoma cells depends on uptake by caveolae-mediated endocytosis. Clin Cancer Res 2009;15:1259–68.
[27] Bradford MM. A rapid and sensitive method for the quantitation of microgram quantities of protein utilizing the principle of protein-dye binding. Anal Biochem 1976;72:248–54.
[28] Reithofer M, Galanski M, Roller A, Keppler BK. An entry to novel platinum complexes: carboxylation of dihydroxoplatinum(IV) complexes with succinic anhydride and subsequent derivatization. Eur J Inorg Chem 2006;13:2612–7.
[29] Aguirre JM, Gutiérrez A, Giraldo O. Simple route for the synthesis of copper hydroxyl salts. J Braz Chem Soc 2011;22:546–51.
[30] Harris AL, Yang X, Hegmans A, Povirk L, Ryan JJ, Kelland L, et al. Synthesis, characterization, and cytotoxicity of a novel highly charged trinuclear platinum compound. Enhancement of cellular uptake with charge. Inorg Chem 2005;44:9598–600.
[31] Williams JW, Qu Y, Bulluss GH, Alvorado E, Farrell NP. Dinuclear platinum complexes with biological relevance based on the 1,2-diaminocyclohexane carrier ligand. Inorg Chem 2007;46:5820–2.
[32] Giandomenico CM, Abrams MJ, Murrer BA, Vollano JF, Rheinheimer MI, Wyer SB, et al. Carboxylation of kinetically inert platinum(IV) hydroxy complexes. An entry into orally active platinum(1V) antitumor agents. Inorg Chem 1995;34:1015–21.
[33] Gang XB, Zhu HF, Shi YB, Tang WX. In vitro binding of an orally active platinum antitumor drug, JM216 to metallothionein. Biometals 2001;14:51–7.
[34] Xiao H, Zhou D, Liu S, Zheng Y, Huang Y, Jing X. A complex of cyclohexane-1,2-diaminoplatinum with an amphiphilic biodegradable polymer with pendant carboxyl groups. Acta Biomater 2012;8:1859–68.
[35] Xiao H, Zhou D, Liu S, Qi R, Zheng Y, Huang Y, et al. Delivery of active DACH-Pt anticancer species by biodegradable amphiphilic polymers using thiol-ene radical addition. Macromol Biosci 2012;12:367–73.